Nanoscale Advances

ROYAL SOCIETY OF CHEMISTRY

PAPER

View Article Online
View Journal | View Issue

Check for updates

Cite this: *Nanoscale Adv.*, 2020, **2**, 4961

Graphene quantum dots in photodynamic therapy†

Jiayi Chen,[a] Wentian Wu,[b] Fangwei Zhang,[b] Jiali Zhang,[b] Hui Liu,[a] Jing Zheng,*[a] Shouwu Guo*[b] and Jingyan Zhang[a]

Received 31st July 2020
Accepted 16th September 2020

DOI: 10.1039/d0na00631a

rsc.li/nanoscale-advances

Graphene quantum dots (GQDs) have shown great promise in a variety of medical applications. Recently, it has been found that GQDs are also beneficial for photodynamic therapy (PDT). However, the findings of GQDs as PDT agents have been controversial in the literature. Herein, we investigate the photoactivity of single-atomic-layered GQDs by examining their ability to generate singlet oxygen ($^1O_2$) under irradiation and their effects on the photoactivity of photosensitizers. We demonstrate that the GQDs with lateral sizes of ~5 or 20 nm are photo-inactive for they cannot generate $^1O_2$ under irradiation of either a 660 nm laser (105 mW cm^{-2}) or a halogen light. Moreover, the GQDs inhibit the photoactivity of two classical photosensitizers, namely, methylene blue and methylene violet. The stronger interaction between the GQDs and the photosensitizer results in greater inhibition of GQDs. Besides, the large-sized GQDs exhibit stronger inhibition than the small-sized GQDs. The inhibitory effect of the GQDs on the photoactivity of photosensitizers is consistent with their photo-cytotoxicity. These results indicate that the single-atomic-layered GQDs are not potential PDT agents, but they may be helpful for photosensitizers by delivering them into the cells. The discrepancy between the current work and the literature is probably associated with the GQDs used.

Introduction

Owing to their high surface area, excellent biocompatibility, and unique chemical and physical properties, graphene quantum dots (GQDs) have shown great potential in bioimaging, drug delivery, biosensing, *etc.*[1–5] Recently, it has been reported that GQDs can also generate singlet oxygen ($^1O_2$) upon irradiation, thus GQDs themselves are potential photodynamic therapy (PDT) agents.[6–14] The electrochemically produced GQDs irradiated with a blue light (470 nm, 1 W) generated $^1O_2$ and other reactive oxygen species, and killed U251 human glioma cells by causing oxidative stress.[6] Ge *et al.* demonstrated that GQDs prepared by a hydrothermal method with polythiophene derivatives as a carbon source could produce $^1O_2$ with a significantly high yield.[8] They believed the $^1O_2$ may be generated *via* two pathways: conventional energy transfer from the excited triplet state (T_1) and the energy transfer from the excited singlet state (S_1) to $^3O_2$.[8] Zhou *et al.* believed that the ability to generate $^1O_2$ and other reactive oxygen species (ROS) by GQDs is closely related to their ketonic carbonyl groups, and the removal of the functional oxygen-containing groups of the GQDs could increase their photostability and lower the photoinduced cytotoxicity of the GQDs.[12] This result, however, is critically dependent on the lateral size and the amount of the peripheral functional groups of the GQDs.

It has also been shown that GQDs can improve the photoactivity of photosensitizers, thus probably are PDT auxiliary agents, which may be similar to the combination of the semiconductor quantum dots with a traditional PDT agent.[15–22] For instance, a nanosystem composed of GQDs with a redox-triggered cleavable PEG shell was designed for the selective recovery of photoactivity of chlorine e6 (Ce6) in a tumor-relevant environment.[18] In this unique system, the GQDs enabled an efficient quench of the fluorescence and $^1O_2$ generation of Ce6. However, once this nanosystem was exposed to a tumor-relevant glutathione environment, the disulfide-linked PEG shell started a reductive cleavage and subsequent detachment from the GQD scaffold, leading to the accelerated release of Ce6 with recovered photoactivity, even though the Ce6 was not bound to PEG.[18] This group latter reported a different system that Ce6 directly bound to the GQDs through a disulfide bond and found that the Ce6–GQDs system displayed considerably stronger quenching ability to the fluorescence of Ce6, but the photoactivity of the Ce6 in the system was recovered in the presence of a reducing agent.[19] Nafiujjaman *et al.* also showed that GQDs enhanced the photoactivity of Ce6 that was loaded through hyaluronic acid (HA).[23] These results indicate that the GQD-based systems can substantially improve the photoactivity of photosensitizers, though the mechanism underneath remains unclear. However, several studies have

[a]*State Key Laboratory of Bioreactor Engineering, Shanghai Key Laboratory of New Drug Design, School of Pharmacy, East China University of Science and Technology, Shanghai, 200237, P. R. China. E-mail: zhengjing@ecust.edu.cn*

[b]*Department of Electronic Engineering, School of Electronic Information and Electrical Engineering, Shanghai Jiao Tong University, Shanghai 200240, P. R. China. E-mail: swguo@sjtu.edu.cn*

† Electronic supplementary information (ESI) available: Experimental data of characterizations of the GQDs, different singlet oxygen detection methods, and EPR data of the GQDs alone after the irradiation, and interaction of GQDs with photosensitizers. See DOI: 10.1039/d0na00631a

Open Access Article. Published on 17 September 2020. Downloaded on 12/5/2025 1:01:18 PM.
This article is licensed under a Creative Commons Attribution-NonCommercial 3.0 Unported Licence.

Open Access Article. Published on 17 September 2020. Downloaded on 12/5/2025 1:01:18 PM.
This article is licensed under a Creative Commons Attribution-NonCommercial 3.0 Unported Licence.

shown that graphene-based materials could quench ROS in many systems.[10,24,25] For instance, Xu *et al.* found that folic acid-modified nanographene oxide quenched the $^1O_2$ generation by cationic porphyrin resulting in a lower phototoxicity.[26]

Herein, we use single-layered GQDs with different sizes to systematically investigate the potential of the GQDs as PDT reagents, including their ability to generate $^1O_2$ and their effect on the photoactivity of photosensitizers.

Experimental section

Materials

The GQDs were prepared from graphene oxide by a photon-Fenton reaction[27] and further separated as described in our previous work.[28] Typically, to obtain differently sized GQDs, the gel electrophoresis method was employed. The aqueous suspension of the as-synthesized GQDs was mixed with 10% glycerine and then injected into the sample well. The sample was run in two steps, a low voltage of 50 V was first applied for 6 min, and then a voltage of 120 V was used for 25 min until the brown band reached the middle of the gel. The different color bands of GQDs were carefully cut out under UV light after the electrophoresis. The incised gel bands were soaked in purified water for 24 h to recover the corresponding GQDs. The resulting GQD solutions were centrifuged and the supernatant was dialyzed to remove the electrolytes.[28] The blue GQD bands were used in this work. Methylene blue (MB), methylene violet (MV), rose bengal (RB), 9,10-anthracenediyl-bis(methylene)dimalonic acid (ADMA), 2,2,6,6-tetramethylpiperidine (TEMP), *N*,*N*-dimethyl-4-nitrosoaniline (RNO), histidine, 1,3-diphenylisobenzofuran (DPBF), singlet oxygen sensor green (SOSG), sodium chloride (NaCl), potassium chloride (KCl), disodium phosphate dodecahydrate ($Na_2HPO_4 \cdot 12H_2O$), potassium dihydrogen phosphate (KH_2PO_4), sodium acetate, acetic acid glacial, ethanol and *N*,*N*-dimethylformamide (DMF) of analytical grade were purchased and used as received.

GQDs were characterized by atomic force microscopy (AFM) in a tapping mode using a Multimode Nanoscope V scanning probe microscopy system (Bruker, USA). TEM images were obtained using a JEM-2010 transmission electron microscope (JEOL, Japan) operating at 200 kV. The samples were prepared by placing the aqueous suspension of GQDs after dialysis on the copper grids and drying under ambient conditions. FT-IR spectra were recorded using an Equinox 55 FT-IR spectrometer (Bruker, Germany). The specimens for FT-IR measurement were prepared by grinding the dried powder of GQDs or GO with KBr together and then compressing into thin pellets. The UV-visible measurements of the samples were performed using a Cary 50 spectrometer (Varian, USA). The fluorescence spectra were recorded using a Cary Eclipse spectrofluorometer (Varian, USA). Electron paramagnetic resonance (EPR) spectra were recorded using a Bruker BioSpin GmbH, with 100 kHz modulation frequency and 1.0 G modulation amplitude at room temperature.

Singlet oxygen detection

A 660 nm laser and a 100 W halogen lamp were used in the experiments, and the light intensity was measured using a photo radiometer (Delta Ohm, Padua, Italy). ADMA was used to detect $^1O_2$ generation by monitoring the absorption changes of ADMA.[29] Photosensitizers and GQDs were mixed in phosphate-buffered saline (PBS: 0.01 M, pH 7.4). In general, ADMA (30 μg mL^{-1}) was added to the sample solution before it was irradiated by light sources. At each predetermined time interval, the absorbance of the sample at 320 nm to 420 nm was recorded. The change in the absorbance of ADMA indirectly reflects the amount of radicals generated by the system, and the change in the absorbance at 380 nm was calculated using the following formula: $\Delta A_{380} = A_0 - A_1$, where A_0 is the absorbance of the sample at 380 nm before irradiation and A_1 after irradiation. The ADMA alone was measured as a control. The ΔA_{380} value for the samples of the GQDs with photosensitizers was calculated as ΔA_{380} (GQDs + photosensitizers) − ΔA_{380} (photosensitizers).

The $^1O_2$ was also detected by the bleaching of *N*,*N*-dimethyl-4-nitrosoaniline (RNO), and its absorbance at 440 nm would be diminished by the presence of $^1O_2$.[30] The solution of photosensitizers and GQDs was mixed with an RNO solution (0.5 μL of 250 μM stock) and 150 μL of histidine (30 mM) solution before irradiation. After irradiation, the absorbance of the sample was recorded at 440 nm.

EPR spectroscopy was also employed to detect $^1O_2$ during irradiation based on the principle that the generated $^1O_2$ by the system reacts with TEMP forming a stable radical adduct TEMPO. Photosensitizers, GQDs, and TEMP (20 mM) were mixed in a phosphate buffer before irradiation.

In vitro PDT experiments

Phototoxicity of photosensitizers, GQDs, and the mixtures of two were measured with human breast cancer cells MCF-7 (purchased from Shanghai Cell Bank of the Chinese Academy of Sciences). MCF-7 cells were cultured in DMEM (high glucose) supplemented with 10% bovine serum and 1% antibiotics (penicillin and streptomycin) at 37 °C in an atmosphere containing 5% CO_2. The viability of MCF-7 cells was assayed using a CCK-8 assay kit (Beyotime Institute of Biotechnology, China). The MCF-7 cells were seeded in 96-well plates at a density of 12 000 cells per well and treated with MB, MV, and GQDs. The cells were subsequently incubated with photosensitizers and GQDs for 24 h. Moreover, the same volume of serum-free DMEM was added to the untreated control group and incubated for the same duration. The cells were then washed twice with PBS and a fresh culture medium was added. All the groups were exposed to a laser beam of 660 nm (600 mW) for 5 min. The cells were incubated for another 24 h, and the standard CCK-8 assay kit was used to measure the cell viabilities. The cytotoxicity of MB, MV, and GQDs under dark conditions was also measured under the same condition without irradiation.

Results and discussion

GQDs cannot generate singlet oxygen

The single-atomic-layered GQDs with different lateral sizes were prepared and characterized according to our previously published work.[27] Fig. 1 shows their AFM images, thickness, and size distributions. About 50% of GQD-1 are about 20 nm in size

 This journal is © The Royal Society of Chemistry 2020

Open Access Article. Published on 17 September 2020. Downloaded on 12/5/2025 1:01:18 PM.
This article is licensed under a Creative Commons Attribution-NonCommercial 3.0 Unported Licence.

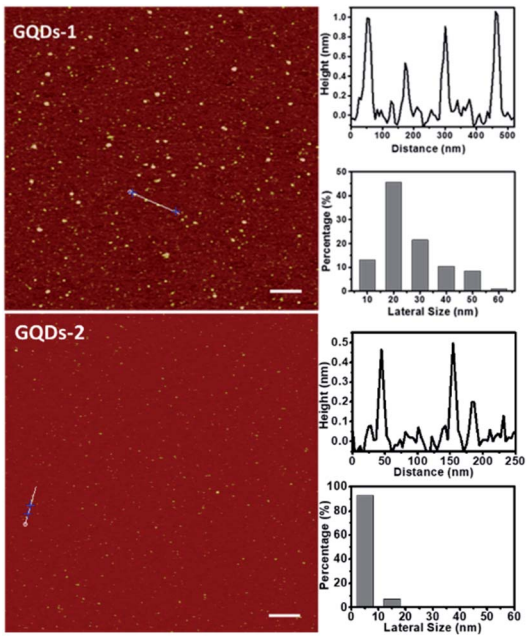

Fig. 1 AFM images of the single-atomic-layered GQDs, their corresponding heights, and size distributions. Top: GQD-1, scale bar is 300 nm. Bottom: GQD-2, scale bar is 200 nm.

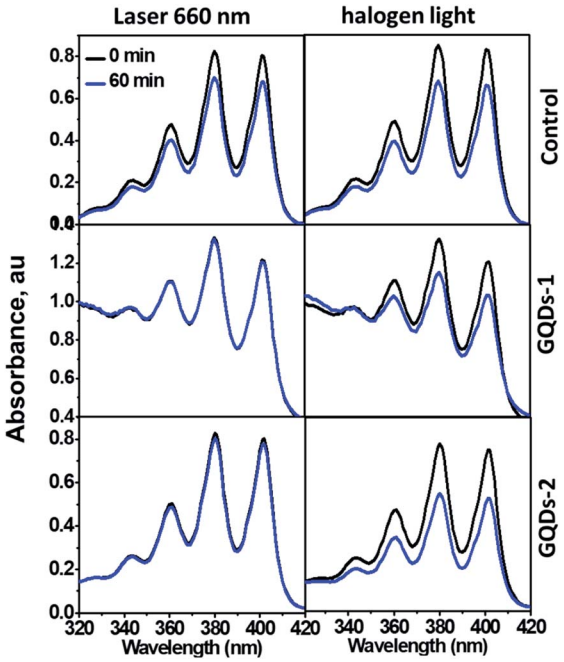

Fig. 2 Generation of $^1O_2$ by differently sized GQDs detected by the ADMA method. Absorption spectra of ADMA in the presence of GQDs with different sizes after irradiation with a laser and halogen light for 60 min. Zero-minute represents the sample before irradiation. Control was ADMA alone under the same conditions. The GQD concentration was 50 μg mL^{-1} for each sample.

and 80% of GQD-2 are ~5 nm in size. In both cases, the heights of the GQDs are all below 1 nm, indicating that they have a single-layered structure. The structural feature and properties of the GQDs were further confirmed by high-resolution TEM images and Raman, UV-vis, fluorescence, and FT-IR spectra, as shown in Fig. S1.† We chose the GQDs with two different sizes because it has been shown that differently sized GQDs have different biocompatibilities, and the number of periphery carbonyl groups, which is primarily determined by the size of the GQDs, is also associated with their photostability.[12,28]

As aforementioned, it has been reported in the literature that owing to the ability of $^1O_2$ generation, GQDs could enhance the photoactivity of the photosensitizers, and thus could be used as PDT reagents, similar to the photosensitizer molecules.[6,7,9–14,31] However, the findings of GQDs as PDT agents or auxiliary PDT agents for photosensitizers are controversial. Therefore, we first investigate whether GQDs themselves have photoactivity, and more specifically, whether they can generate $^1O_2$.

Several often-used methods of $^1O_2$ detection were first examined. Most $^1O_2$ detection methods are monitoring the changes in absorbance or fluorescence intensity of the $^1O_2$ detecting reagents, including DPBF,[9,13,22] SOSG,[11,17–19] ADMA,[29] and RNO.[30] Among them, DPBF is insoluble in aqueous solutions, its aqueous suspension with GQDs generates a false positive signal, which might be due to the organic solvent used (Fig. S2a†). The GQDs quench the fluorescence of SOSG, resulting in a false negative result (Fig. S2b†). Based on these observations, we employed water-soluble reagents ADMA and RNO as $^1O_2$ detecting reagents in the following experiments. Here, $^1O_2$ was also detected by electron paramagnetic resonance spectroscopy (EPR) using a $^1O_2$ trapping agent, TEMP, as described in the Experimental section.

Fig. 2 showed the ADMA absorbance in the presence of GQDs (decrease in absorption indicates the generation of $^1O_2$). Because the GQDs exhibited weak absorption at long wavelengths (Fig. S1a†), we used both a 660 nm laser and a halogen lamp as irradiation sources. No obvious change was observed in the GQD suspensions with different irradiation time periods (15–60 min), indicating that both GQD-1 and GQD-2 cannot generate $^1O_2$. Conversely, GQDs can prevent the photodegradation of ADMA caused by laser irradiation (left panel in Fig. 2), as evidenced by the unchanged absorbance of ADMA compared with the control. In contrast, the photodegradation of ADMA caused by the irradiation of halogen light was not efficiently prevented by the GQDs, possibly due to the wide wavelength range of the halogen light (400–800 nm, right panel in Fig. 2). Failure to generate $^1O_2$ by the GQDs was further confirmed by EPR trapping experiments with TEMP, a $^1O_2$ tapping agent. TEMPO signal was observed neither in the GQD-1 aqueous suspension nor in the GQD-2 aqueous suspension after irradiation. These observations are consistent with the work by Li *et al.*, who found that the GQDs efficiently quenched the generation of $^1O_2$ by Ce6.[18] However, our finding is contradicted to the GQDs prepared by hydrothermal treatment of polythiophene, which exhibited excellent $^1O_2$ generation with a quantum yield of 1.3.[31] This discrepancy is possibly caused partially by their GQDs that hybridized with nitrogen and sulphur. The nitrogen-doped GQDs have been shown with higher ^1O production ability than the GQDs reported previously.[11]

Open Access Article. Published on 17 September 2020. Downloaded on 12/5/2025 1:01:18 PM.
This article is licensed under a Creative Commons Attribution-NonCommercial 3.0 Unported Licence.

Can GQDs enhance the activity of the photosensitizer?

The GQDs themselves are not photoactive, is it still possible that they can enhance the photoactivity of the photosensitizers as reported in the literature?[18–21] To answer this question, the photoactivity of two photosensitizers, namely, methylene blue (MB) and methylene violet (MV) were measured in the presence of GQD-1 and GQD-2. MB and MV are phenothiazinium dyes with a strong absorbance in the range of 550–700 nm and significant quantum yields, which make them very effective photosensitizers.[32,33] The photoactivity of MB or MV alone was measured separately under the same condition as a control (Fig. S3†).

Fig. 3 shows the $^1O_2$ production of MB and MV in the presence of different amounts of GQD-1 (black traces) and GQD-2 (red traces). To better compare the effect of the GQDs on the two sensitizers, the concentrations of MB and MV were chosen in such a way to ensure they generate a similar amount of $^1O_2$. The decrease in the ΔA_{380} nm indicated that the $^1O_2$ generation by MV or MB were both inhibited by GQD-1 and GQD-2. The inhibition was also dependent on the GQD concentration, the higher the concentration of the GQDs present, the stronger the inhibition observed. The inhibition to both photosensitizers by GQD-1 (black traces) was more effective than that by GQD-2 (red traces). For instance, with 20 μg mL^{-1} of GQDs, GQD-1 reduced the $^1O_2$ production of MB by 4-fold compared to GQD-2. The inhibition of GQDs to the $^1O_2$ production of the MB and MV was also confirmed by the decrease in the EPR signal intensity of TEMPO, a product of $^1O_2$ with TEMP, with the increase in the concentration of the GQDs (Fig. S4†). The inhibition of the GQDs to MB and MV was either by directly inhibiting the generation of $^1O_2$ or by quenching the generated $^1O_2$. In the former case, the interaction between the GQDs and the photosensitizers is critical. Since MB and MV both are planar molecules (Fig. S5†), they can interact with GQDs *via* π–π stacking and electrostatic interactions.[26] As expected, owing to their larger sizes, GQD-1 interacts with MV and MB more effectively than the small-sized GQD-2; therefore, less $^1O_2$ were generated in the presence of GQD-1 than in the presence of GQD-2. Previously, we and others found that GO and GQDs can quench oxygen reactive species such as OH$^\bullet$, $O_2^{\bullet-}$, and $^1O_2$,[10,26,34,35] and it was also reported that GQDs could quench DPPH radicals.[10] However, we cannot differentiate between the inhibition and quenching of $^1O_2$ by the GQDs at this stage, they could occur concurrently, or one of them is dominant.

To understand further the inhibition of GQDs to the photoactivity of MB and MV, interactions between GQDs and MB, MV were examined by the fluorescence measurement. It has been generally accepted that GQDs can quench the fluorescence of small molecules or single-stranded nucleic acid *via* π–π stacking.[1,36,37] Fig. S5† shows that in the presence of GQDs, the fluorescence of MB and MV were quenched as expected, and the binding constants (k_b) of MB and MV can thus be obtained. k_b for MB is 10-fold lower than that of MV for both GQD-1 and GQD-2, revealing that MB binds to the GQDs more tightly than MV. Different binding abilities of MB and MV to GQDs are unexpected because MB and MV have very similar planar chemical structures (insets in Fig. S5†). However, MB and MV have different functional groups, which suggests that other weak interactions such as electrostatic interaction may also contribute to their interaction with the GQDs. This assumption was supported by the result of the photoactivity of MB and MV in the presence of GQD-1 at different pH values. The electrostatic interaction between GQD-1 and MB or MV can be affected by pH because the protonation states of the functional groups in MB and MV are different at different pH values. As shown in Fig. 4a, the photoactivities of MV at pH 5 and 7.4 were quite similar in the presence of GQD-1, suggesting that none or a very weak electrostatic interaction was involved in the interaction between MV and GQDs. In contrast, the photoactivity of MB in the presence of GQDs at pH 5 was higher than that at pH 7.4, while the photoactivity of MB alone is independent of pH. The pH-dependent photoactivity of MB/GQD-1 indicated that when pH was 5, the electrostatic interaction between the carboxyl groups of GQD-1 and the amine group of MB was weak, and some MB was mobile, and thus, its photoactivity was relatively

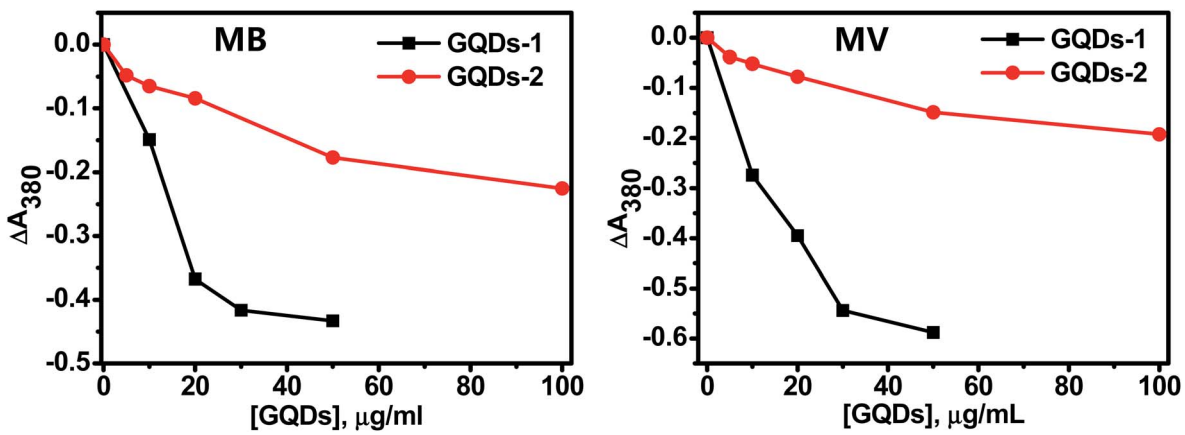

Fig. 3 Effect of the GQDs on the photoactivity of MB and MV. The photoactivity of MB and MV was measured under the irradiation of a 660 nm laser for 15 min. The concentration of MB was 0.5 μM, MV was 2 μM, GQD-1 was 50 μg mL^{-1}, and GOD-2 was 100 μg mL^{-1}. The absorbance change of ADMA at 380 nm was calculated according to the formula described in the Experimental section.

 This journal is © The Royal Society of Chemistry 2020

Open Access Article. Published on 17 September 2020. Downloaded on 12/5/2025 1:01:18 PM.
This article is licensed under a Creative Commons Attribution-NonCommercial 3.0 Unported Licence.

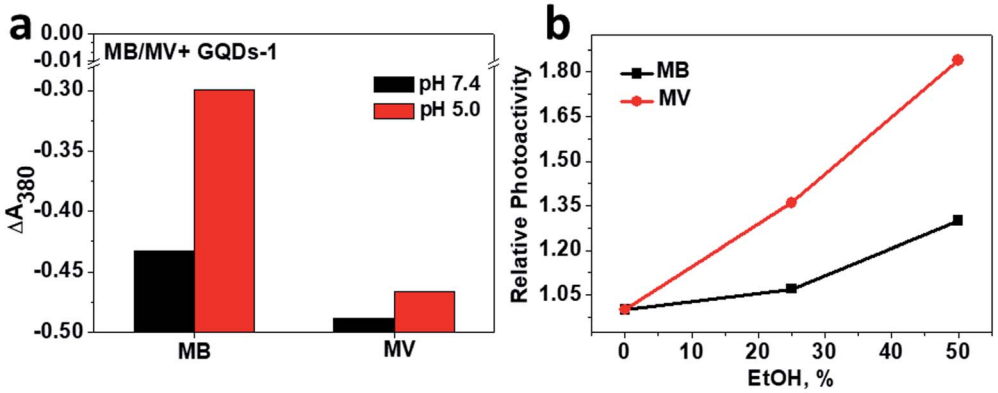

Fig. 4 (a) Photoactivity of MV and MB in the presence of the GQD-1 (50 μg mL^{-1}) at pH 7.4 (PBS buffer) and pH 5.0 (acetate buffer). The concentration of MB was 0.5 μM and MV was 2 μM. (b) Relative photoactivity of MV/GQD-1 and MB/GQD-1 in the presence of ethanol. All samples were measured after 15 min of irradiation with a 660 nm laser.

high. When the pH was neutral, this interaction was relatively strong, thus the inhibition of GQD-1 to the photoactivity of MB increased. This assumption was further supported by the photoactivity of MB and MV with GQD-1 in the presence of ethanol, which affects the π–π stacking between photosensitizers and GQDs, but interferes less to the electrostatic interaction between them.[1] As shown in Fig. 4b, in the presence of 50% ethanol, the photoactivity of MV/GQD-1 increased much more than that of MB/GQD-1, because the hydrophobic interaction is the major driving force between MV and GQDs. These results together indicated that the inhibition of GQD-1 to the photoactivity of MB and MV depends on the extent of their interaction. GQD-1 interact with MB more strongly, thus their inhibition to the photoactivity of MB is more severe than to that

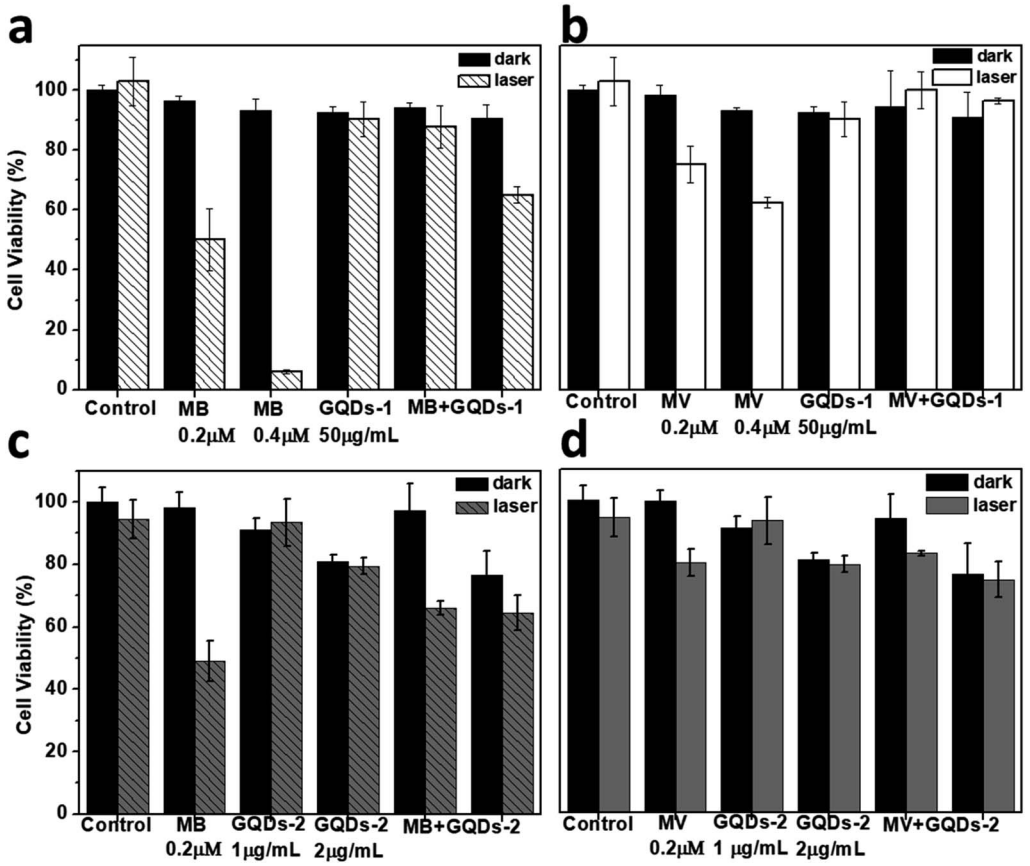

Fig. 5 Phototoxicity of MB, MV, GQDs, MB/GQDs, and MV/GQDs. (a) MB with GQD-1, (b) MV with GQD-1, (c) MB with GQD-2, and (d) MV with GQD-2. The MCF-7 cells with these additives were first incubated for 24 h and then irradiated with a 660 nm light (210 mW cm^{-2}) for 5 min. The concentrations of GQDs, MV, and MB were used as indicated.

Open Access Article. Published on 17 September 2020. Downloaded on 12/5/2025 1:01:18 PM.
This article is licensed under a Creative Commons Attribution-NonCommercial 3.0 Unported Licence.

of MV. This conclusion was also supported by the effect of GQDs on the photoactivity of another typical photosensitizer, rose bengal (RB). Fig. S6a† show that the inhibition of both GQD-1 and GQD-2 to the photoactivity of RB was almost negligible because the interaction between GQDs and RB is relatively weak (Fig. S6b†). The interaction of GQDs with these photosensitizers also suggested that the GQDs in the systems with Ce6 or other photosensitizers were carriers for the photosensitizers, as reported in the literature,[6–14] which is similar to the GQDs in drug delivery.[1–5,18–21] Collectively, these results indicated that GQDs inhibit the $^1O_2$ production of photosensitizers, which is presumably due to the energy transfer between the GQDs and the photosensitizers.[10,26,34,35,38]

Inhibition of the GQDs to the photoactivity of MB and MV at the cellular level

We further examined the inhibition of the GQDs to the photoactivity of MB and MV at the cellular level by monitoring their photo-cytotoxicity under irradiation. As shown in Fig. 5a and b, in the presence of the GQD-1, the photo-cytotoxicity of MB and MV was inhibited after irradiation compared to the cells incubated with MB or MV alone. For instance, the cell viability with MB (0.2 μM) was recovered from 50% to ~80% in the presence of GQD-1. Owing to its low photoactivity, the inhibition of GQD-1 to the phototoxicity of MV is less obvious. The inhibitory effect of GQD-2 is much weaker (Fig. 5c and d), which is consistent with the weak interaction between GQD-2 and MB or MV (Fig. S5†). These results reinforced the observation at the molecular level that GQDs inhibit the photoactivities of photosensitizers.

The current results are different from the literature that GQDs were reported to be able to enhance the photoactivity of Ce6 or other photosensitizers.[15–22] The discrepancy could be caused by the difference in the GQDs used. In many reported works, the GQDs were prepared by the hydrothermal method with organic compounds used as carbon sources, and in most cases, they were carbon dots (CDs), instead of the single-atomic-layered GQDs.[13,14,17,31,39] This assumption is consistent with their much stronger fluorescence than the single-atomic-layered GQDs. In some other cases, the as-prepared GQDs were prepared using graphite by the classic method; no further separation was performed.[7,9] The lateral size of these as-prepared GQDs often ranges from several to hundred nanometres, and multi-layered GQDs also co-exist.[6,7,19,22] The interaction of these GQDs with photosensitizers must be complicated.

Nevertheless, photosensitizers can attach to single-atomic-layered GQDs or carbon dots *via* weak interactions, thus they could be taken into the cells as a cargo, and their cellular accumulation is likely to be improved. This is probably the major reason that the photoactivity of the GQDs/photosensitizer systems was improved compared to the photosensitizer alone.

Conclusions

We examined the photoactivity of single-atomic-layered GQDs with different sizes under irradiation of a laser and halogen light to explore their potential as PDT agents. We also studied the effect of the GQDs on the photoactivity of photosensitizers as PDT auxiliary agents. We first excluded several methods of $^1O_2$ detection that cause false positive or negative results due to the intrinsic properties of their interactions with the GQDs of the reagents. Using the two confirmed methods, we found that the single-atomic-layered GQDs of size ~5 or 20 nm cannot generate $^1O_2$. On the contrary, we found that the GQDs quenched the photoactivity of photosensitizers MB and MV, and this is closely associated with the interaction between the GQDs and photosensitizers that often have aromatic rings. The stronger interaction between them leads to a stronger inhibition of the GQDs to the photosensitizers. However, the interaction between the GQDs and photosensitizers makes it possible for the GQDs to deliver those attached photosensitizers into the cells or other biological systems. Based on these findings, we infer that the primary role of the GQDs in many GQD–photosensitizer systems reported in the literature is to deliver the photosensitizers into the cells. The discrepancy of our current result with some studies reported in the literature is most probably associated with the GQDs used in the experiments. Many of them are not single-atomic-layered GQDs, but they are carbon dots that have different properties compared to the GQDs.

Conflicts of interest

There are no conflicts to declare.

Acknowledgements

This research was carried out with financial support from National Science Foundation of China (No. 21671065), the State Key Laboratory of Bioreactor Engineering (No. 2060204), the Shanghai Committee of Science and Technology (No. 11DZ2260600).

Notes and references

1 C. Wang, C. Wu, X. Zhou, T. Han, X. Xin, J. Wu, J. Zhang and S. Guo, *Sci. Rep.*, 2013, **3**, 2852.
2 X. Wang, X. Sun, J. Lao, H. He, T. Cheng, M. Wang, S. Wang and F. Huang, *Colloids Surf., B*, 2014, **122**, 638–644.
3 X. Zhao, L. Yang, X. Li, X. Jia, L. Liu, J. Zeng, J. Guo and P. Liu, *Bioconjugate Chem.*, 2015, **26**, 128–136.
4 J. Liu, L. Cui and D. Losic, *Acta Biomater.*, 2013, **9**, 9243–9257.
5 D. Iannazzo, A. Pistone, M. Salamo, S. Galvagno, R. Romeo, S. V. Giofre, C. Branca, G. Visalli and A. Di Pietro, *Int. J. Pharm.*, 2017, **518**, 185–192.
6 Z. M. Markovic, B. Z. Ristic, K. M. Arsikin, D. G. Klisic, L. M. Harhaji-Trajkovic, B. M. Todorovic-Markovic, D. P. Kepic, T. K. Kravic-Stevovic, S. P. Jovanovic and M. M. Milenkovic, *Biomaterials*, 2012, **33**, 7084–7092.
7 B. Z. Ristic, M. M. Milenkovic, I. R. Dakic, B. M. Todorovic-Markovic, M. S. Milosavljevic, M. D. Budimir, V. G. Paunovic, M. D. Dramicanin, Z. M. Markovic and V. S. Trajkovic, *Biomaterials*, 2014, **35**, 4428–4435.

 This journal is © The Royal Society of Chemistry 2020

Open Access Article. Published on 17 September 2020. Downloaded on 12/5/2025 1:01:18 PM.
This article is licensed under a Creative Commons Attribution-NonCommercial 3.0 Unported Licence.

8 J. Ge, M. Lan, B. Zhou, W. Liu, L. Guo, H. Wang, Q. Jia, X. Huang, H. Zhou, X. Meng, P. Wang, C.-S. Lee, W. Zhang and X. Han, *Nat. Commun.*, 2014, **5**, 4596.
9 S. P. Jovanovic, Z. Syrgiannis, Z. M. Markovic, A. Bonasera, D. P. Kepic, M. D. Budimir, D. D. Milivojevic, V. D. Spasojevic, M. D. Dramicanin, V. B. Pavlovic and B. M. Todorovic Markovic, *ACS Appl. Mater. Interfaces*, 2015, **7**, 25865–25874.
10 Y. Chong, C. Ge, G. Fang, X. Tian, X. Ma, T. Wen, W. G. Wamer, C. Chen, Z. Chai and J. J. Yin, *ACS Nano*, 2016, **10**, 8690–8699.
11 W. S. Kuo, H. H. Chen, S. Y. Chen, C. Y. Chang, P. C. Chen, Y. I. Hou, Y. T. Shao, H. F. Kao, C. L. Lilian Hsu, Y. C. Chen, S. J. Chen, S. R. Wu and J. Y. Wang, *Biomaterials*, 2017, **120**, 185–194.
12 Y. Zhou, H. Sun, F. Wang, J. Ren and X. Qu, *Chem. Commun.*, 2017, **53**, 10588–10591.
13 D. Zhang, L. Wen, R. Huang, H. Wang, X. Hu and D. Xing, *Biomaterials*, 2018, **153**, 14–26.
14 M. Thakur, M. K. Kumawat and R. Srivastava, *RSC Adv.*, 2017, **7**, 5251–5261.
15 M. R. Detty, S. L. Gibson and S. J. Wagner, *Chem. Inf.*, 2004, **35**, 3897.
16 D. van Straten, V. Mashayekhi, H. S. de Bruijn, S. Oliveira and D. J. Robinson, *Cancers*, 2017, **9**, 19.
17 K. Habiba, J. Encarnacion-Rosado, K. Garcia-Pabon, J. C. Villalobos-Santos, V. I. Makarov, J. A. Avalos, B. R. Weiner and G. Morell, *Int. J. Nanomed.*, 2016, **11**, 107–119.
18 Y. Li, Z. Wu, D. Du, H. Dong, D. Shi and Y. Li, *RSC Adv.*, 2016, **6**, 6516–6522.
19 D. Du, K. Wang, Y. Wen, Y. Li and Y. Y. Li, *ACS Appl. Mater. Interfaces*, 2016, **8**, 3287–3294.
20 L. Zhou, L. Zhou, X. Ge, J. Zhou, S. Wei and J. Shen, *Chem. Commun.*, 2015, **51**, 421–424.
21 M. Nafiujjaman, V. Revuri, H.-K. Park, I. K. Kwon, K.-J. Cho and Y.-k. Lee, *Chem. Lett.*, 2016, **45**, 997–999.
22 Y. Cao, H. Dong, Z. Yang, X. Zhong, Y. Chen, W. Dai and X. Zhang, *ACS Appl. Mater. Interfaces*, 2017, **9**, 159–166.
23 M. Nurunnabi, K. Parvez, M. Nafiujjaman, V. Revuri, H. A. Khan, X. Feng and Y.-k. Lee, *RSC Adv.*, 2015, **5**, 42141–42161.
24 I. L. Christensen, Y. P. Sun and P. Juzenas, *J. Biomed. Nanotechnol.*, 2011, **7**, 667.
25 J. Zhao, B. Zhang, C. Yu, Y. Liu, W. Wang and J. Li, *Carbon*, 2016, **109**, 487–494.
26 J. Xu, F. Zeng, H. Wu, C. Yu and S. Wu, *ACS Appl. Mater. Interfaces*, 2015, **7**, 9287–9296.
27 X. Zhou, Y. Zhang, C. Wang, X. Wu, Y. Yang, B. Zheng, H. Wu, S. Guo and J. Zhang, *ACS Nano*, 2012, **6**, 6592–6599.
28 F. Zhang, F. Liu, C. Wang, X. Xin, J. Liu, S. Guo and J. Zhang, *ACS Appl. Mater. Interfaces*, 2016, **8**, 2104–2110.
29 Y. Tang, H. Chen, K. Chang, Z. Liu, Y. Wang, S. Qu, H. Xu and C. Wu, *ACS Appl. Mater. Interfaces*, 2017, **9**, 3419–3431.
30 A. Sahu, W. I. Choi, J. H. Lee and G. Tae, *Biomaterials*, 2013, **34**, 6239–6248.
31 J. Ge, M. Lan, B. Zhou, W. Liu, L. Guo, H. Wang, Q. Jia, G. Niu, X. Huang, H. Zhou, X. Meng, P. Wang, C. S. Lee, W. Zhang and X. Han, *Nat. Commun.*, 2014, **5**, 4596.
32 M. Derosa and R. Crutchley, *Coord. Chem. Rev.*, 2002, **233–234**, 351–371.
33 A. O'Connor, W. Gallagher and A. Byrne, *Photochem. Photobiol.*, 2009, **85**, 1053–1074.
34 C. Youngnam, K. Hyunjin and C. Yongdoo, *Chem. Commun.*, 2013, **49**, 1202–1204.
35 C. Youngnam and C. Yongdoo, *Chem. Commun.*, 2012, **48**, 9912–9914.
36 L. Zhuang, J. T. Robinson, S. Xiaoming and D. Hongjie, *J. Am. Chem. Soc.*, 2008, **130**, 10876–10877.
37 Z. Liu, X. Sun, N. Nakayama-Ratchford and H. Dai, *ACS Nano*, 2007, **1**, 50–56.
38 E. Yoo, T. Okata, T. Akita, M. Kohyama, J. Nakamura and I. Honma, *Nano Lett.*, 2009, **9**, 2255–2259.
39 A. P. Kauling, A. T. Seefeldt, D. P. Pisoni, R. C. Pradeep, R. Bentini, R. V. B. Oliveira, K. S. Novoselov and A. H. Castro Neto, *Adv. Mater.*, 2018, **30**, e1803784.